Recent developments in optofluidic-surface-enhanced Raman scattering systems: Design, assembly, and advantages

Yin Yin
Department of Physics, Southeast University, Nanjing 211189, China
Teng Qiu[a)]
Department of Physics, Southeast University, Nanjing 211189, China
Wenjun Zhang
Department of Physics and Materials Science, City University of Hong Kong, Kowloon, Hong Kong
Paul K. Chu[b)]
Department of Physics and Materials Science, City University of Hong Kong, Kowloon, Hong Kong

(Received 4 May 2010; accepted 12 July 2010)

Surface-enhanced Raman scattering (SERS) coupled with micro- or nanofluidics integrated into optofluidic devices offer many advantages over conventional SERS conducted under static conditions. Higher reproducibility, larger intensity, as well as greater enhancement can be achieved by efficient mixing of analytes and SERS enhancers under a continuous flow. Progress and advances in the past 10 years, including the design of channels and efficient mixing conditions, assemblies of SERS substrates for optimal enhancement, and advantages of optofluidic-SERS analysis, are reviewed. Recent results show that optofluidic-SERS effectively overcomes many of the difficulties and limitations plaguing conventional SERS and the novel technique has enormous application potential.

I. INTRODUCTION

A. Technological motivation and scientific underpinnings

Raman scattering is a powerful technique to determine the structure of molecules and crystals. On the basis of interactions between photons and molecules, Raman scattering can be used to obtain information on chemical structures, identify substances according to the characteristic spectral patterns, and determine quantitatively or semiquantitatively the amount of a substance in a sample.[1] Raman scattering refers to the phenomenon that involves excitation of a molecule by inelastic scattering of a photon.[2] When substances are irradiated by light, the photons may be absorbed or scattered or pass straight through. In the case when the energy of a photon matches the energy gap between the ground state and an excited state of a molecule, the photon may be absorbed and excite the molecule to the higher energy state. Alternatively, scattering of photon can occur if its energy does not correspond to the energy gap. In this case, if the photons are scattered with very small frequency changes, the scattering process is regarded as elastic scattering, which is the dominant process called Rayleigh scattering. If nuclear motion is induced during the scattering process, energy is transferred between the molecule and photon. As a result, this process involves excitation of a molecule by inelastic scattering and the energy of the scattered photon is different due to the different vibrational modes. This is Raman scattering. Although Raman scattering was discovered more than 80 years ago,[3] it made great strides only after the advent of laser technology, design of efficient filters to reduce Rayleigh scattering, and development of extremely sensitive detectors.[4] Nowadays, spectroscopic techniques used to detect structurally informative vibrations in molecules are based on infrared absorption and Raman scattering.[5] Compared to infrared spectroscopy, the use of Raman spectroscopy has been hampered for a long time due to problems associated with sample degradation, fluorescence interference, and most importantly low efficiency caused by the small scattering cross sections.[6] The detection sensitivity rendered by Raman scattering is poor compared to fluorescence emission and infrared absorption.

Surface-enhanced Raman scattering (SERS), first observed in 1974 by Fleischman, has drawn substantial attention and become a useful analytical tool.[5,7] It has been demonstrated as a promising way to overcome the poor efficiency of the inelastic scattering processes and the weak signals inherent to traditional Raman spectroscopy. The detection sensitivity of nanoparticles can be enhanced by up to 6–10 orders of magnitude by using SERS.[8–11] The enhancement rendered by SERS is commonly explained

Address all correspondence to these authors.
[a)]e-mail: tqiu@seu.edu.cn
[b)]e-mail: paul.chu@cityu.edu.hk
DOI: 10.1557/jmr.2010.18

by two theoretical models, electromagnetic and chemical enhancements.[12,13] The former is considered to be the dominant one and used to explain most SERS phenomena.[14] According to the electromagnetic enhancement mechanism, the metal surface irradiated by a laser beam couples with the electromagnetic radiation.[15] The oscillations of the conduction band electrons confined on the nanometer-sized metal surface, a process called surface plasmon resonance, result in a larger number of scattered photons.[16] The frequency of the surface plasmon resonance strongly depends on the dielectric properties of the metals such as Cu, Ag, Au, and alkalis and the surface morphology of the substrate such as size and shape of particles, which are considered to be much smaller than the incident optical wavelength.[17] Compared to other optical detection methods, SERS based on metal nanoparticles provides many analytical advantages including higher sensitivity, surface specificity, and fluorescence quenching.[18] Furthermore, it opens up a new way to detect multiple analytes simultaneously because of the sharpness of the spectral signals, which may have full width at half-maximum values of as small as 1 nm.[19]

B. Brief history

SERS is closely linked to nanoscience. The SERS intensity decreases significantly if the structures are either much larger than ~100 nm or much smaller than ~10 nm, such as the cases for nanoparticles, nanorods, and/or nanowires. The SERS enhancement mainly depends on the geometric configuration of the nanostructures. That is, the enhancement is induced by the state of aggregation that generates the corresponding plasmon resonance. In addition, it is possible to obtain an enormous Raman enhancement at "hot spots" on aggregated particle clusters.[20–22] However, it is difficult to predict where the hot spots occur, and the degree of SERS enhancement thus varies with the distributions of these hot spots. Moreover, the poor reproducibility caused by different particle sizes and inhomogeneous aggregation does not bode well for quantitative analysis.[23,24] One way to overcome these difficulties is by incorporating microfluidic systems into SERS.[25–27] In general, the advantages of microfluidic-SERS are the reduced sample size, shorter reaction time, and improved yield compared to conventional techniques conducted under static conditions.[28–30] With a continuous flow and homogeneous mixing between the analytes and metal nanoparticles in the micro- or nanochannels, higher reproducibility and stability can be attained. When the flow rates are kept constant, the same conditions can be repeated for a series of measurements. An additional advantage of fluidics is that local sample heating can be prevented as the molecules exposed to the laser are constantly refreshed due to the fluid flow.

C. Roadmap

Integration of optical detection technologies and microfluidic systems into "optofluidic" devices is an emerging area.[31] Optofluidics refer to a class of optical systems synthesized with fluids.[32] Although microfluidic chips have made it possible to integrate multiple fluidic tasks on a chip, most optical components such as the light source, sensors, lenses, and waveguides, remain off the chip. In contrast, optofluidic integration combines optics and microfluidics on the same chip by building the optics from the same fluidic toolkit. In an optofluidic system, the optical properties of the nanoparticles and analytes can be changed by manipulating the fluids. In addition to the benefits offered by microfluidic-SERS, one of the greatest advantages of optofluidic systems is the greater ability to obtain reproducible SERS enhancement factors and consequently more reliable quantitative results via the formation of consistent SERS-active clusters or regular nanopatterning substrates.[6] In this review, we focus on the advantages of SERS-based detection conducted in conjunction with micro- or nanofluidics and integrated into optofluidic devices. Although a number of reviews have been written on the development of optical detection methods, reviews about the advantages of microfluidic-SERS or optofluidic-SERS are rare. In this work, the optofluidic-SERS detection technology is first overviewed, followed by a general description of how to fabricate chips for SERS detection and ways to obtain stable and enhanced SERS signals. The emphasis is placed on the advantages of optofluidic-SERS analysis such as quantitative detection and determination of multiple analytes. We will also describe recent developments and finally, future developments and prospects of optofluidic-SERS are discussed.

II. OVERVIEW OF OPTOFLUIDIC-SERS

In conventional SERS performed under static conditions, the main problem is the poor reproducibility caused by the different particle sizes and inhomogeneous distribution of molecules on the metal surface. To improve the situation, SERS under fluidic conditions was proposed about 20 years ago.[33] In recent years, microfluidic technologies have made great strides and opened up the possibility of using very small quantities of samples and reagents to carry out efficient, low-cost separation and detection at high resolution and sensitivity.[34]

In general, there are two main types of SERS techniques on microfluidic chips, namely homogeneously and heterogeneously. In the first way, the targets are absorbed onto the metal nanoparticles in a solution acting as the Raman enhancers.[35] Large field enhancement is achieved in systems consisting of nearly touching particles, such as aggregated or close-packed colloids.[36,37] This method not only provides all the advantages of homogeneous

reactions, such as faster reaction rate and relative ease of implementation, but also offers some extra benefits including enhanced uniformity and repeatability. However, the detection sensitivity is relatively low due to the dispersed Raman enhancers in the solution phase. In the heterogeneous method in which the solution phase targets interact with the SERS-active substrates such as roughened metallic electrodes, metal substrates, enhanced detection sensitivity, and reproducible SERS signals can be achieved. A number of Ag and Au SERS substrates have therefore been introduced.[38–41] Despite these advantages, it takes a long time for the molecules to diffuse to the SERS-active sites leading to low sample concentrations and making it difficult to obtain uniform distributions of molecular adsorption from the analysis sites. In some cases, these surface phase systems also complicate chip fabrication and subsequent integration with microfluidic devices.

Recently, optofluidic systems based on SERS devices, which combine the advantages of homogeneous and heterogeneous detection techniques, have been used to acquire reproducible SERS signals with higher sensitivity and reduced reaction time.[42] Optofluidic systems, in which optics and microfluidics are used synergistically to synthesize novel functionalities, can offer many advantages such as small sample size, fast mixing, and improved analytical performance.[43] In particular, much interest has been devoted to the liquid core optical ring resonator (LCORR).[42,44–46] Figures 1(a) and 1(b) illustrate the operating mechanism. The laser confined by a waveguide traverses the circumference of the capillary and when the sample flows through the LCORR capillary, the analytes with silver nanoparticles yield SERS signals with very high sensitivity and reproducibility. In this system, not only does the LCORR capillary provide a means for sample movement, but also the ring resonator offers a Raman intensity enhancement mechanism. Huh et al.[47] have reported an optofluidic-SERS device consisting of an SERS-active substrate and polydimethylsiloxane (PDMS) microfluidic chip. The SERS-active PDMS substrate comprises ordered nanotube structures of Au/Ag/Au with uniform packing constructed by metal evaporation through a mask of a nanoporous anodized alumina (AAO) membrane. Using the noble SERS substrate, this chip-based approach can generate sensitive SERS signals for quantitative analysis. Choi et al.[48] have presented an optofluidic SERS-compact disk (CD) platform in which preconcentration of target molecules is accomplished via accumulation of adsorbed molecules on the SERS-active sites by repeating a "filling–drying" cycle of the assay solution [see Fig. 1(c)]. After 30 cycles, stable and high-sensitivity SERS signals are detected from rhodamine 6G. In addition, precipitation of gold nanoparticles (GNPs) by $CuSO_4$ has been introduced to produce uniform, high-throughput, high-sensitivity, and large-area SERS substrates on the optofluidic CD platform, which will be further discussed in Sec. IV.

III. FABRICATION OF OPTOFLUIDIC-SERS SYSTEMS

A. Design of channels for efficient mixing conditions

There are several excellent reviews on the development of methods and materials for microfluidic chips.[49–52] A number of new optofluidic approaches for the purpose of integrating SERS detection systems with micro- or nanofluidics have been proposed. Here, we focus on the microchannel design in the microfliudic chips where efficient mixing can be accomplished to induce fast adsorption of analytes onto the metal nanoparticles or SERS-active structures leading to reproducible and stable SERS detection.

Conventional SERS suffers from the variable mixing time, different scattering geometry, localized heating, and unresolved photodissociation[23] In contrast, optofluidic-SERS provides higher reproducibility, which would be difficult to achieve under static conditions because of unpredictable aggregation of colloids containing nanoparticles with different sizes and inhomogeneous distribution of analytes on the surface of the metal nanoparticles. Furthermore, by taking advantage of the continuous flow and excellent heat dissipation, controllable and uniform distribution of "hot spots" can be achieved in optofluidic-SERS systems. Consequently, efficient mixing, which contributes to stable and reproducible SERS signals, is crucial to the design of microchannel structures in microfluidic devices.

A significant feature in the fluid flow in a microchannel is the laminar flow regime in which parallel streams flow along each other. Mixing takes place only when diffusion and turbulent flow occurs.[53] Mixing by diffusion only is rarely used because of the long mixing length and long time[54]; consequently, there are several approaches to reduce the mixing length enabling more rapid mixing of the fluids. Generally speaking, there are two ways in which efficient mixing with a high transport rate can be obtained (i) passive mixing in which microgeometries are applied to increase the interfacial area between the analytes and nanoparticles, and (ii) active mixing in which extra active components are integrated into the channels. In passive mixing, multiple streams are divided and mixed within a fluid network. Figures 2(a) and 2(b) show the Y-shaped and T-shaped channels with several miscible fluid streams for more efficient mixing. Passive mixing can also be carried out by introducing obstacles into the microchannels, and various patterns and blocking arrays have been designed. Figure 2(c) displays a zigzag channel in the microfluidics/SERS system and Fig. 2(d) depicts a microfluidic chip with pillar-array obstacles to enhance the mixing efficiency and

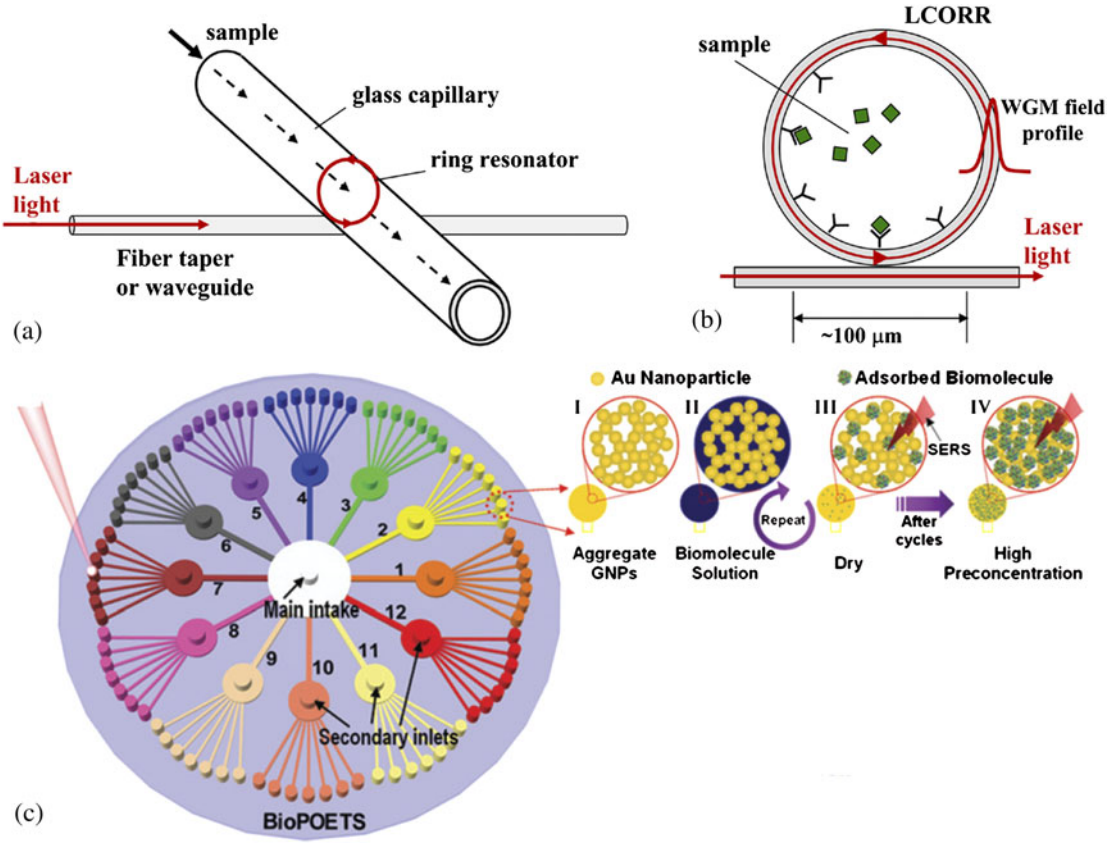

FIG. 1. (a) Schematic illustration of the LCORR in the microchannel. (b) When the sample is captured at the inner surface of the LCORR, it interacts with the whispering gallery modes evanescent field.[46] (c) Optofluidic SERS-CD platform with high-throughput sample preparation. The mechanism of preconcentration involves four steps. I: Fabrication of SERS-active sites, II: Injection of a sample solution; III: Adsorption of target molecules onto the SERS-active site during drying process prior to SERS measurement; IV: Accumulation of the adsorbed molecules by the repetition of the steps II and III.[48]

SERS signals. Active mixing by combining pulsed electric field and pumps is more efficient and easier to control; however, mixing may complicate the fabrication of microfluidic devices.[59] Figure 3 shows that bubbles can be used to achieve a high degree of fluid transport and mixing enhancement in a chamber microfluidic device.[60] Oddy et al.[61] have developed an electrokinetic instability micromixing process to rapidly stir micro- and nanoliters of solutions to enhance mixing of the targets in the solution. The Raman enhancers yield greater detection sensitivity in microfluidic bioanalytical applications.

B. Assemblies of SERS substrates for optimal enhancement

The progress in SERS heretofore hinges on developments in nanoscience and nanotechnology, especially optimized nanostructures of metal substrates such as nanoparticles, nanoclusters, nanowires, and nanoholes.[62,63] Originally, substrates found to exhibit SERS are quite limited and they mainly include electrochemically modified electrodes, colloids, and island films. Compared to the random distribution of nanostructures on a roughened metal surface in the past, the substrates nowadays are fabricated on the nanoscale with features that can deliver high reproducibility and sensitivity. Fabrication of the proper SERS substrates is important to obtain a homogeneous size and shape distribution of the particles that can generate large enhancement in the Raman signals from the target molecules. Nanostructured metal substrates can be prepared by either self-assembly or directed assembly. The former is also called the bottom-up approach. By controlling the temperature, concentration, and other factors, nanospheres, nanowires, and nanocubes can be synthesized. The technique is used widely due to the low cost, simple equipment, straightforward process, and stable signals. Luo et al.[64] have used an AAO template as a nanosieve to arrange Au nanoparticles into a nanonet to achieve layer assembly using the pressure difference method. Figure 4 shows the self-assembled nanoparticles on the AAO templates at the same pressure difference. Figure 4(a) reveals the netlike assembly formed on the 200-nm AAO template and Fig. 4(b) displays the layer coating assembly formed on the 20-nm AAO.

Kang et al.[65] have developed a new Au nanowire–Au nanoparticle conjugated system in which the nanostructures are fabricated by self-assembly of Au nanoparticles onto an atomically smooth surface of an Au nanowire via

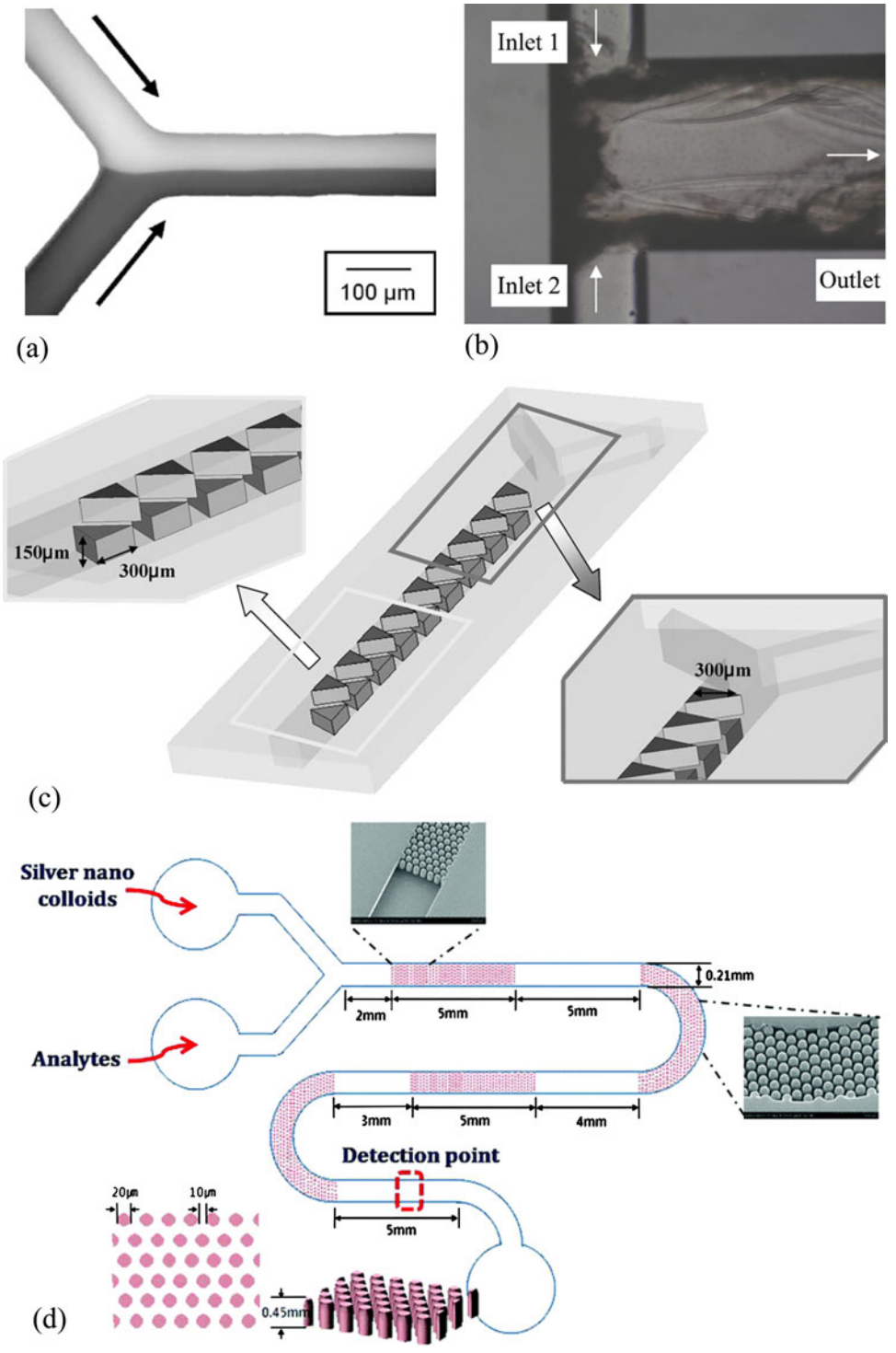

FIG. 2. Passive mixing in the microfluidic channel. (a) Y-shaped channel[55]; (b) T-shaped channel[56]; (c) zigzag-shaped channel[57]; (d) pillar array microfluidic channel.[58]

biotin–avidin interactions (Fig. 5). Here, hot spots are generated at the Au nanowire–nanoparticles junctions and the target molecules are absorbed by these hot spots yielding enhanced Raman signals. The number of the Au nanoparticles attached to the nanowire is proportional to the concentration of avidin. We have also developed a nanotechnique to assemble silver nanocrystals on an active coating and control the gaps precisely down to the sub-10-nm regime. This coating exhibits a high Raman signal enhancement factor due to a very high density of both Ag nanoparticles (~1.8×10^{12} cm^{-2}) and hot junctions (~5.4×10^{12} cm^{-2}) (see Fig. 6).[66]

We have recently reported another convenient nanotechnique to assemble hemispherical silver nanocap arrays on an AAO membrane template as a robust and cost-effective SERS substrate. This geometry emits a high Raman signal due to the periodical hexagonal arrangement and precise gap control between the nanostructures in the sub-10-nm range. The surface structure can further be tuned to optimize the enhancement factor by varying the AAO fabrication and silver deposition parameters. Figure 7 shows the scanning electron microscopy (SEM) images of the silver-coated AAO membranes produced using different Ag sputtering time of 15 and 20 min together with the corresponding SERS spectra. The intensity of the rhodamine 6G Raman signal decreases when the sputtering time is increased due to particle aggregation between adjacent silver nanocaps when the size becomes large.

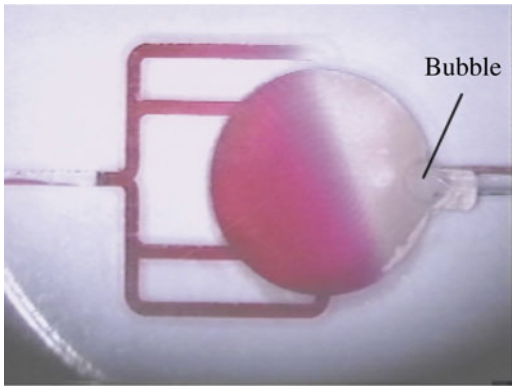

FIG. 3. Schematic drawing of bubble-induced mixing in a microfluidic chip.[60]

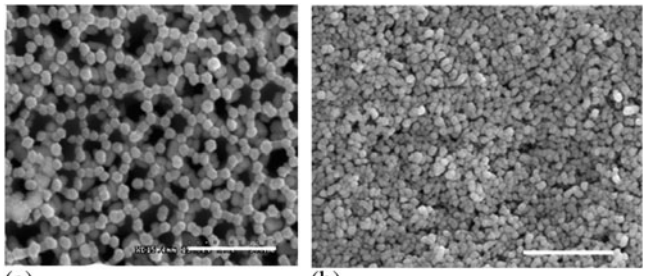

FIG. 4. Assemblies of Au nanoparticles via the pressure difference method: the dimension bar is 500 nm for all. (a) SEM image of the netlike assembled colloidal Au nanoparticles on 200-nm pores of AAO membrane; (b) particle coatings assembly on 20-nm pores of alumina membrane.[64]

More direct assembly substrates are now available thanks to rapid developments in nanofabrication technology, especially lithographic techniques. This approach is also known as "top-down"[68] in which the structure is directly written on the substrate by an electron beam. More uniform SERS substrates with nanostructures fabricated in the desired locations in orderly patterns, which yield higher sensitivity than single molecules, can be produced by this method.[69,70] As aforementioned, the major problem plaguing quantitative analysis is the difficulty to come up with SERS substrates with well-defined and uniform properties, but nanolithographic techniques offer a solution and quantitative SERS analysis is now possible. In addition, it opens up other applications involving optically active nanostructures integrated into a microfluidic system.[38] Sackmann et al.[71] have described a novel gold active substrate in which the gold nanostructures are prepared on a silicon wafer using regular particle arrays produced by electron-beam lithography (EBL). Here, crystal violet is chosen as the test sample and the reproducibility is evaluated using the same substrate several times after cleaning. Figure 8 shows an electron microscopy image of the resulting nanostructures used in the SERS experiments.

IV. ADVANTAGES OF OPTOFLUIDIC-SERS ANALYSIS

A. Quantitative detection

As described in Sec. I, quantitative SERS analysis is challenging despite its discovery more than 30 years ago,[72,73] but quantitative analytical protocols using optofluidic systems, especially SERS analysis of analytes in a microfluidic channel, can offer rapid and highly sensitive detection. The low sensitivity and poor reproducibility

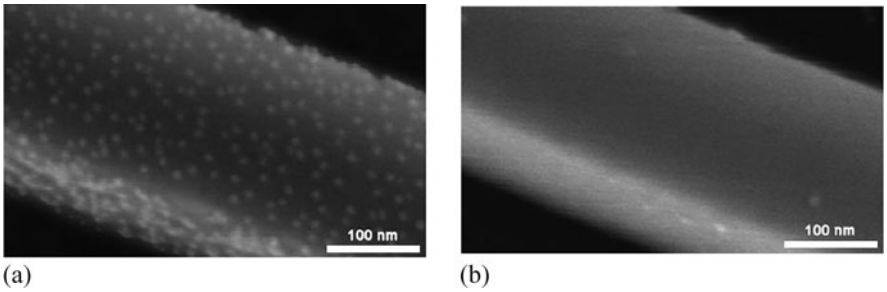

FIG. 5. SEM images of Au nanowire–nanoparticles conjugated system. (a) Au nanowire–nanoparticles system by biotin-avidin interaction with avidin concentration of 10^{-6} M; (b) nonspecifically bound Au nanoparticles onto Au nanowire without avidin. Evenly distributed Au nanoparticles are clearly seen in (a), while few Au nanoparticles are identified in (b).[65]

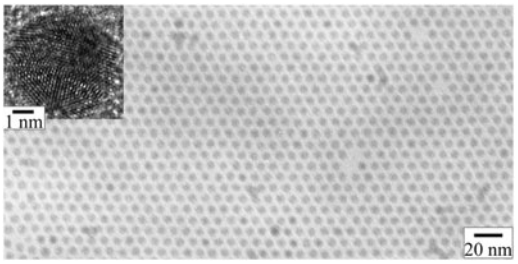

FIG. 6. Bright-field transmission electron microscopy (TEM) image of a self-assembled monolayer of silver nanocrystal superlattice. The inset shows the high-resolution TEM image of a typical silver nanocrystal.[66]

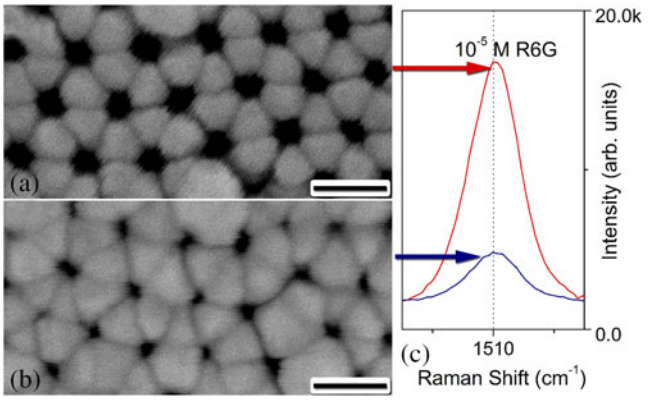

FIG. 7. SEM images obtained from the silver-coated AAO membranes formed using different Ag sputtering times of (a) 15 min and (b) 20 min, respectively. Scale bar: 100 nm. Both the PAA membranes are formed at a constant direct current voltage of 40 V. (c) SERS spectra of rhodamine 6G adsorbed silver-coated AAO membranes correspond to those in (a) and (b), demonstrating the intensity variation of the SERS signal at 1510 cm^{-1}.[67]

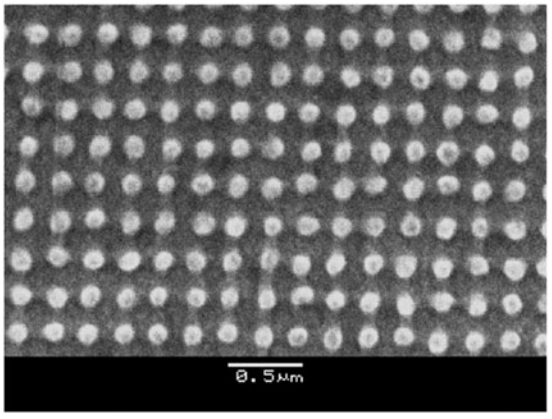

FIG. 8. SEM image of the gold nanostructure used for the SERS experiment. The gold nanostructure was produced by EBL. The distance between the nanodots is 240 ± 5 nm, their diameter is 125 ± 5 nm, and their height is ~25 nm.[71]

inherent to conventional SERS are improved by the flowing fluids in the microchannels. In addition, precise control of the experimental conditions can be accomplished by adopting a highly efficient micromixer. Generally, three factors must be considered in quantitative SERS measurements, namely the wavelength of the laser, SERS-active enhancer, and internal standards.[74] In SERS, the laser wavelength chosen to excite plasmons on the surface of the colloids should match that of the SERS-active enhancers. During aggregation of the colloids, interactions among particles increases scattering, but on the other hand, these interactions may lead to the formation of nanoparticles with different sizes and different absorption maxima and bandwidths causing the spectra to red shift.[75] For this reason, a broad wavelength range is expected from aggregated colloids in a particular measurement.

Ackermann et al.[76] have reported quantitative detection of gradient-driven concentration fluctuations of two different drugs in a SERS microfluidic system in which a citrate-reduced silver colloid serves as the SERS enhancer. The ultraviolet-visible (UV-vis) absorption spectrum in Fig. 9(a) discloses one narrow band at 413 nm. The SERS spectra acquired using a laser wavelength of 532 nm from the colloid with inhomogeneous particle sizes and shape distributions are depicted in Fig. 9(b). Alternatively, if they are deposited onto the structured substrates, the wavelength must be carefully chosen because of the heterogeneous conditions. As aforementioned, the SERS-active enhancers can be categorized as metal nanoparticle colloids or solid SERS-active substrates. The former boasts simple preparation, high enhancement, and low cost. The main advantages of solid substrates are their controllable shape design, which enhances the flexibility in target adsorption. However, the reproducibility is not good because the enhancing ability tends to degrade with time and the degradation rates vary from batch to batch. The ability to obtain reproducible and stable SERS signals depends on whether good size, shape, and distribution uniformity can be achieved during colloid aggregation. In this respect, in conventional SERS detection even under the same conditions, the colloids vary in size and shape thereby yielding variable degrees of SERS enhancement and irreproducible results.[77] In the optofluidic systems, more reproducible conditions can be achieved with the aid of the flowing fluids. The ability to operate within a continuous flow regime, generate homogeneous mixing conditions within the microchannels, and achieve reproducible conditions over a large area benefits quantitative SERS-based analyses.[78]

Cialla et al.[79] describe two reproducible gold SERS-active substrates with the nanodiamond or nanostar structures and apply EBL to accomplish fast sampling and high reproducibility (see Fig. 10). Here, droplets of an aqueous sample solution are placed onto the SERS-active substrates. The samples are subsequently placed in a humidity-controlled chamber for slow drying and a highly homogeneous distribution of analyte molecules can be produced across the array.

In SERS, the enhancement variations due to laser power fluctuations and different diffusion conditions

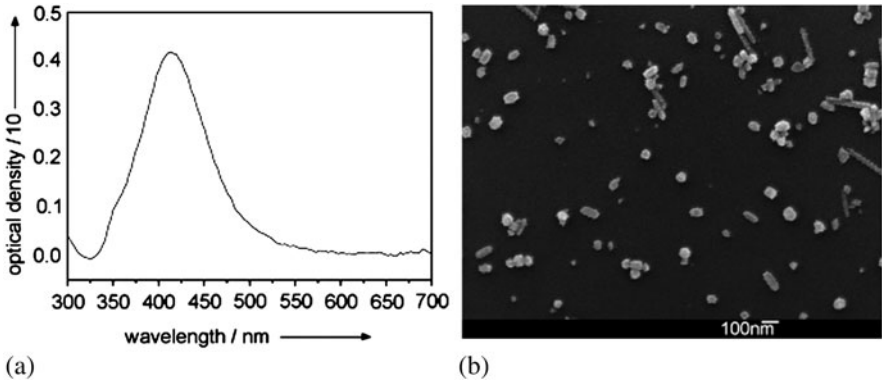

FIG. 9. (a) UV-visible absorption spectrum of silver colloid; (b) SEM image of the respective colloid with an inhomogeneous size and shape distribution.[76]

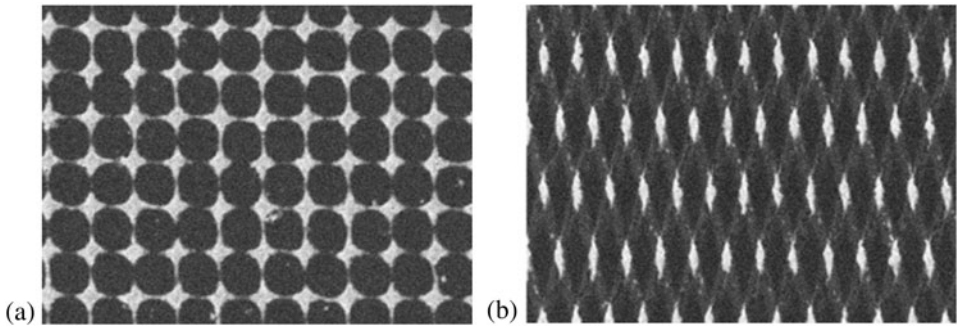

FIG. 10. SEM images of lithographically prepared substrates with a high-grade reproducibility. (a) Gold nanostar structures (period 250 nm); (b) gold nanodiamond structures (period 200 nm).[79]

and substrates make it impossible to accurately calibrate the absolute Raman intensities versus concentrations as required by quantitative analyses. Consequently, standardized production of solid substrates and use of colloids produced in a standard way are imperative to quantitative measurements. However, it is more difficult to find an internal standard due to the complex surface chemistry of metal particles. In the microfluidic systems, good reproducibility can be achieved due to the continuous fluid flow, which reduces the fluctuations in the enhancing media and experimental conditions. In some cases, quantifiable data based on the absolute areas under the emission bands can be obtained.[80] Despite these benefits, different types of internal standards are still necessary to eliminate the fluctuations in the laser power and to correct for minor optical variations. The optimized internal standard must be similar to the molecular structure of the analytes and possess the same relative enhancement factors. The spectra of the internal standard should be measured independently to provide a noninterfering spectral region. Finally, the spectral intensity of the internal standard should be consistent regardless of the amount of analytes. Marz et al.[81] have used respective isotopomers as internal standards to quantitatively determine nicotine by SERS using a PDMS microfluidic channel. In the microchannels, high SERS reproducibility can be achieved because errors caused by differences in sample diffusion in the scattering geometries are avoided. Here, nicotine-d4 is used as the internal standard (see Fig. 11) and this method normalizes the errors induced by aging and differences in the SERS enhancement. No further calibration steps are required and quantitative SERS detection of nicotine can be achieved. Jung et al.[82] have also reported rapid and highly sensitive detection of nicotine using a microfluidic system and SERS detection. Figure 12(a) shows the intensity of the strongest band of nicotine at 1030 cm^{-1} normalized to the reducing agent, hydroxylamine, which shows a peak at 1360 cm^{-1} and is used as the internal standard. Figure 12(b) depicts the linear relationship over the range 0–100 ppm with a correlation coefficient R of 0.998.

A microfluidic system for trace analysis of malachite green (MG) has been described by Lee et al.[83] MG is widely used as a fungicide and antiseptic but has been banned by the U.S. Food and Drug Administration because it is carcinogenic and genotoxic.[84,85] In SERS detection using a fluidic channel, efficient mixing between MG molecules and silver nanoparticles is achieved due to the more consistent geometries and good heat dissipation rendered by the mobile fluids. The results are thus more

reproducible than those obtained using the static mode. Signals arising from low parts per billion (ppb) concentrations of MG can be measured and the detection limit is in fact below 1–2 ppb, which is comparable to that achieved by liquid chromatography–mass spectrometry (LC–MS). Here, acetonitrile is chosen as the internal standard, which yields a strong band without interferences. Figure 13(a) shows the SERS spectra acquired from solutions with different concentrations of MG from 1 to 100 ppb in a PDMS microfluidic channel. The characteristic Raman peak of MG at 1615 cm^{-1}, which increases with MG concentrations, is quantitatively monitored. To correct the Raman signal variability due to batch-to-batch fluctuations, the peak of MG at 1615 cm^{-1} is normalized to the acetonitrile peak at 2258 cm^{-1}, which is the internal standard. The calibration curve in Fig. 13(b) demonstrates a good linear relationship between the peak area ratio (I1615/I2258) and concentrations. These results suggest that highly sensitive and quantitative determination of analytes is possible by coupling SERS with microfluidics.

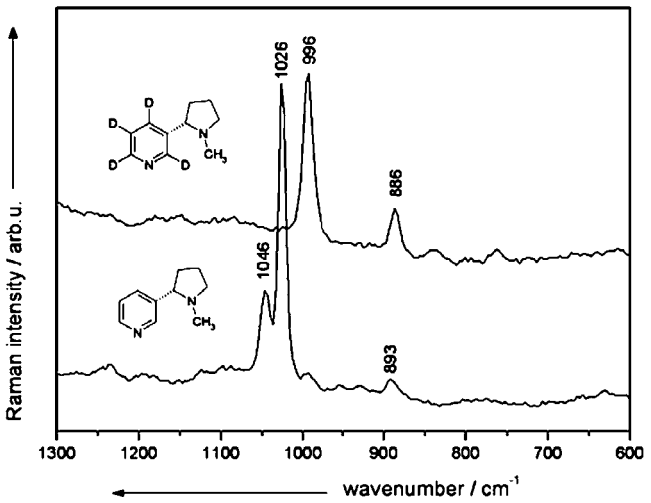

FIG. 11. SERS spectra of nicotine and nicotine-d4. Nicotine-d4 is chosen as an internal standard.[81]

B. Memory effect

The optofluidic device offers a simple system and rapid analysis. By optimizing the continuous flow and mixing, it is possible to generate substantial enhancement. Furthermore, this is the condition under which stable and intense signals with excellent reproducibility and high sensitivity can be achieved when homogenously mixed colloids and SERS-active enhancers are maintained. Although the degree of mixing in the microfluidic channel is better at a smaller flow rate, the reproducibility decreases due to the memory effect produced by deposition of nanoparticle aggregates onto the channel walls. This memory effect degrades the sensitivity and reproducibility. There has been interest in a droplet-based flow cell system coupled with sensitive optical detection due to advantages such as high speed, low sample volumes, and good detection efficiency.[86–91] In droplet microfluidics, droplets are generated and manipulated within an immiscible carrier fluid in the microchannels allowing high-throughput analysis on the single molecule level. Being embedded in the droplets, the individuality and integrity of the samples can be retained.

It has been reported that a two-phase liquid/liquid segmented system prevents nanoparticle aggregates from sticking to the channel surface. The two-phase segmented system generally comprises a carrier such as oil that encapsulates and mobilizes the nanoliter-sized droplets, each of which represents a single sample. Because of the presence of a thin layer with a continuous phase, the droplets do not contact the channel surface and memory effects can be circumvented. In addition, unsupervised online measurements can be conducted over a longer period of time without needing washing steps. Strehle

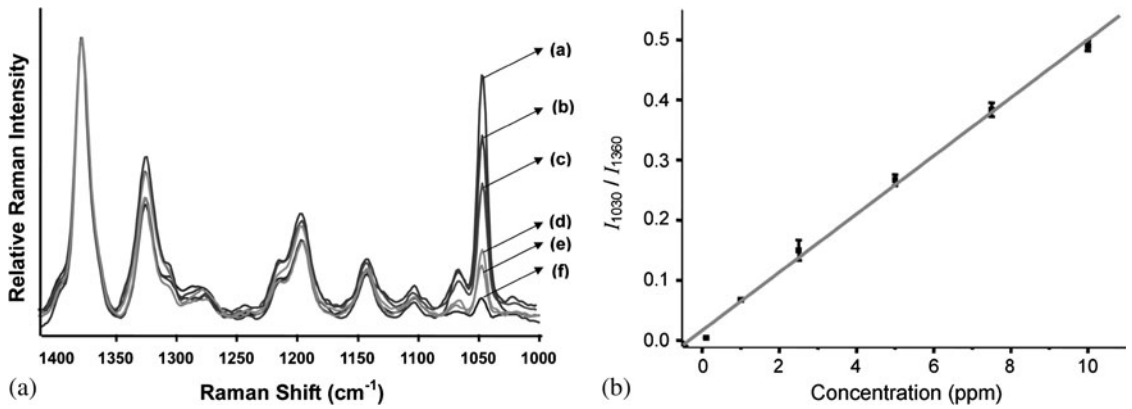

FIG. 12. (a) Concentration-dependent SERS spectra for varying concentrations of nicotine in the microfluidic channel: (a) 10 ppm, (b) 7.5 ppm, (c) 5.0 ppm, (d) 2.5 ppm, (e) 1.0 ppm, and (f) 0.1 ppm. However, the hydroxylamine peak at 1360 cm^{-1} does not change along with the concentrations therefore it is chosen as the internal standard; (b) variations of the peak area ratio (I1030/I1360) as a function of nicotine concentration (correlation coefficient, $R = 0.998$).[82]

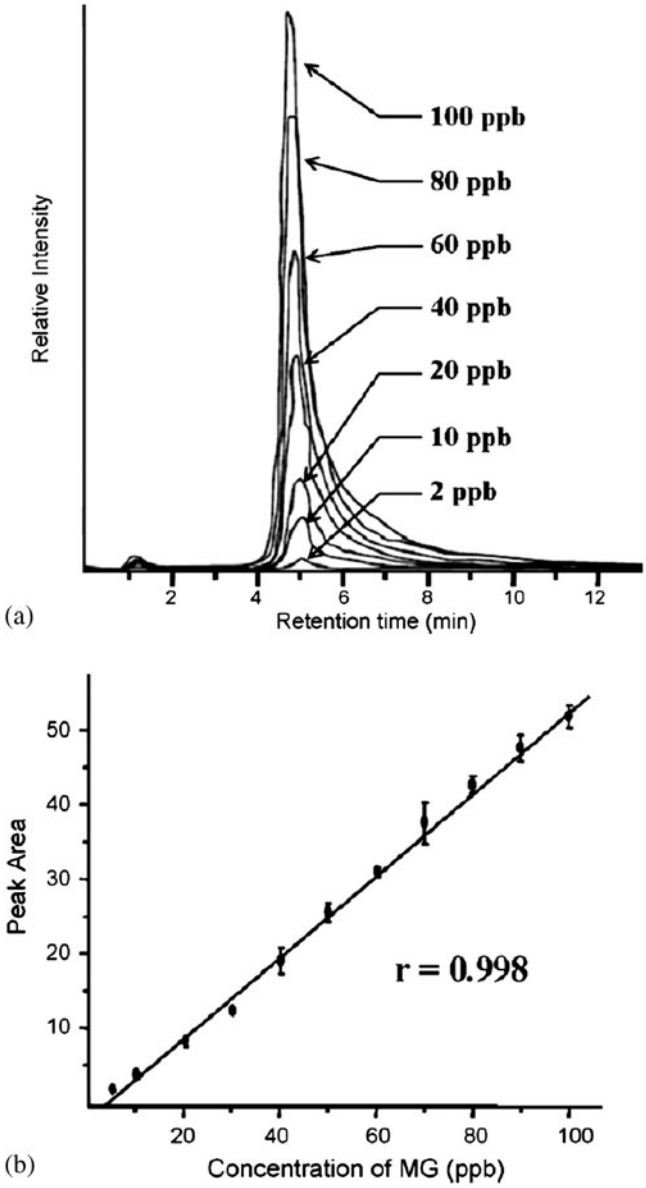

FIG. 13. (a) SERS spectra for varying concentrations of MG in a PDMS microfluidic channel. The concentration ranges from 1 to 100 ppb; (b) variations of MG peak area at 1615 cm^{-1} of SERS spectra as a function of MG concentration (correlation coefficient, $R = 0.993$).[83]

et al.[92] have developed a droplet-based liquid/liquid microsegmented flow system and demonstrated highly reproducible SERS analysis of crystal violet. Here, the channel of the microchip is filled with lipophilic tetradecane and the crystal violet-containing droplets along with SERS enhancers are surrounded by oil. No SERS spectrum can be detected from the crystal violet when probing the microchannels with a laser, demonstrating the absence of memory effects on the channel walls. Figure 14(a) shows the intensity of Raman spectra versus measurement time. Neither the SERS (1621 cm^{-1}) nor tetradecane (1303 and 1442 cm^{-1}) signals can be seen from spectrum A in Fig. 14(b) after 80 s. This spectrum is produced from colloids containing only a water droplet, corroborating that because of the oil film on the surface of the aqueous droplet, there is no deposition of either GNPs or analyte molecules on the microchannels.

Another droplet-based microfluidics, two-phase segmented system is used for efficient mixing and fluid control to provide fast and sensitive SERS detection of mercury (II) ions, which are detrimental to human health and the environment.[93] High-sensitivity determination of mercury (II) ions, is achieved by SERS with rhodamine B (RB) being the medium. The SERS signal of RB increases significantly when it is absorbed on GNPs due to electromagnetic and chemical enhancement factors. However, a decrease in the observed SERS signal may occur because a multitude of RB molecules are released from the metal surface in the presence of mercury (II) ions. Quantitative determination of mercury (II) can be performed by calculating the peak area of RB in the SERS spectrum. Figure 15 illustrates the structure and operation of the device. The aqueous solutions consist of an RB-adsorbed GNPs colloidal solution and a mercury (II) ion solution. The oil film, which acts as the carrier fluid, controls the droplet size by varying the ratio of the aqueous-to-oil flow rates. Because of the presence of the continuous oil layer, memory effects are absent and localization of reagents within discrete and encapsulated droplets enhances mixing and minimizes residence time thereby yielding high analytical throughput and reproducible results.

C. Aggregation of metal nanoparticles

Active enhancers can be generally classified as nanoparticles on solid substrates and colloidal nanoparticles. The former requires complex equipment and fabrication and a long time is needed for the analytes to diffuse to the SERS-active substrates. In contrast, the second type of SERS enhancer, colloids of metal nanoparticles, especially Au and Ag, is used more often[94,95] due to advantages such as homogeneous mixing, ease of manipulation, and inexpensive experiments. When incorporated into an optofluidic device, the poor reproducibility stemming from the metal nanoparticles in the solution can be circumvented. As the fluid flows into the microchannels, the SERS signals from different aggregates are accumulated and averaged and therefore it is relatively easy to improve the detection reproducibility. Here, colloid aggregation with high efficiency and stability prior to SERS measurement plays an important role in the improved SERS activity.[40,96] Controlled aggregation of metal nanoparticles associated with the formation of reproducible metal clusters is believed to be important to the enhancement.

Additional aggregation agents acting as particle–particle linking mediators in the aggregation of metal nanoparticles have been extensively studied. Generally speaking, chloride,

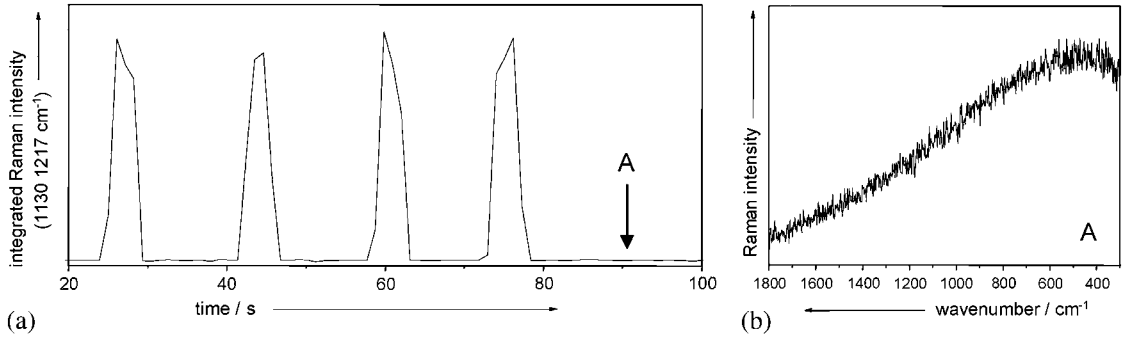

FIG. 14. (a) Peaks representing the integrated Raman intensity abruptly disappear (see left panel), when stopping the flow during the measuring period. (b) In the segments (position A), which now consist of pure colloid without any crystal violet, neither an SERS spectrum nor a tetradecane signal can be detected.[92]

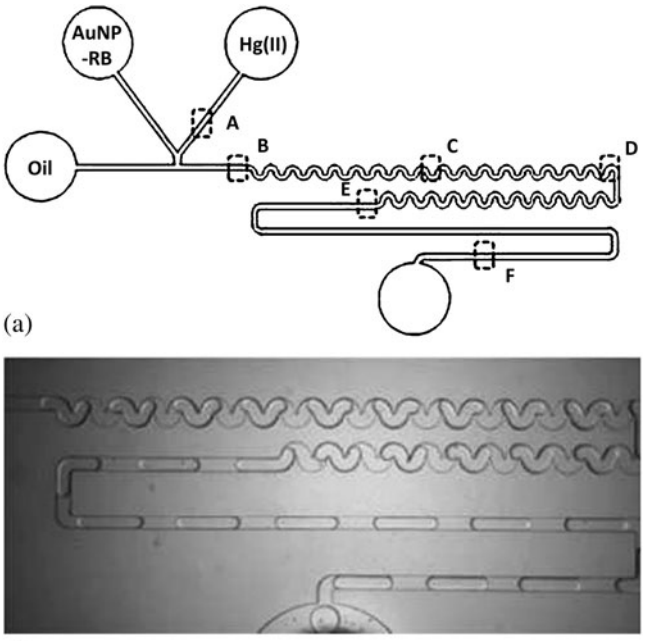

FIG. 15. (a) Schematic representation of the channel pattern used to create droplets; (b) photograph of the assembled device in operation.[93]

nitrate, perchlorate, and polylysine are used as aggregation agents.[97] Cyrankiewicz et al.[98] describe an efficient SERS system using metal colloids plus aggregating agents of HCl, KCl, and HCl. The absorption spectra from the metal nanoparticles show that the SERS enhancement factors vary significantly with the type and concentration of the aggregating agent. Yang et al.[99] have investigated the aggregation behavior and self-assembly mechanism of gold colloids generated by the addition of cetyltrimethylammonium bromide (CTAB) and 11-mercaptoundecanoic acid (MUA). With the aid of MUA, which can diminish the linking function of CTAB, excessive aggregation of the CTAB-modified gold colloids can be prevented. Sulfur species on the surface of the gold particles effectively link the aggregates as demonstrated by Schwartzberg et al.,[100] thereby allowing easy binding and detection of rhodamine 6G. Guingab et al.[101] have developed a new method with dipicolinic acid (APD) as the neutral species added to silver colloids to replace the negative charges caused by the adsorbed anions on the metal particles. The silver colloids exhibit a single extinction band at 385 nm due to resonant excitation of plasma oscillations in the confined electron gas of the particles.[102] There is a single maximum at about 400 nm with increased absorbance because of the higher concentrations of silver particles over time. Moreover, introduction of APD changes the shape of the silver colloid absorption spectrum due to the aggregation of silver particles and appearance of another peak at a longer wavelength indicating the presence of the aggregates. Choi et al.[48] chose $CuSO_4$ as the aggregation agent of gold colloids to acquire high SERS enhancement for rhodamine 6G, because the higher charge on Cu^{2+} induces stronger aggregation. The aggregates formed by $MgCl_2$ are compared to those induced by $CuSO_4$. Figure 16(a) shows the SEM images of the aggregates induced by $CuSO_4$ or $MgCl_2$. $CuSO_4$ is observed to generate aggregates with a higher degree of branching and more two-dimensional surface coverage than $MgCl_2$. Figure 16(b) depicts the SERS spectra of rhodamine 6G and the observed SERS intensity at 1509 cm^{-1} is 5 to 6 times higher in the case of $CuSO_4$ than $MgCl_2$. The results prove that Cu^{2+} is better than other divalent ions to obtain enhanced SERS intensity.

In the optofluidic device, a high degree of aggregation of metal nanoparticles can be achieved with the aid of a flow cell and extra manipulation such as optical components and metallic electrodes. Wang et al.[103] have fabricated an optofluidic device to obtain fingerprint information of proteins at concentrations of nanograms per liter in minutes. The GNPs acting as the SERS enhancers are mixed with the analyte solution. The size is larger than the depth of the nanochannel so that the GNPs are trapped and form clusters at the entrance of the nanochannel, as shown in Figs. 17(a) and 17(b). A high concentration of analytes is found around the gold clusters due to the capillary force contributing to the high detection sensitivity. Figures 17(c) and 17(d) show the aggregation of GNPs within 3 and 12

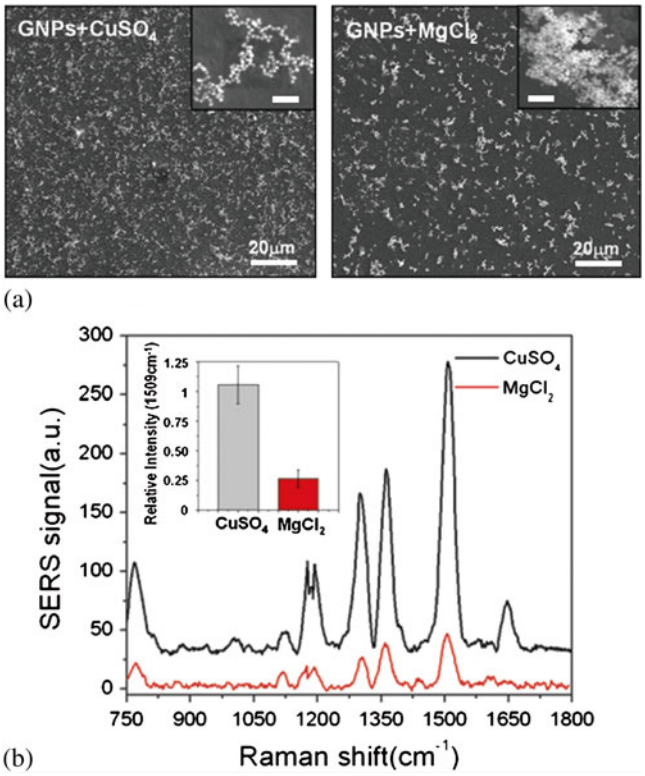

FIG. 16. Effect of different aggregating agents to SERS spectra. (a) SEM images of the GNPs based on aggregation agents, $CuSO_4$ and $MgCl_2$. Despite the same volume of GNPs used, the coverage of $MgCl_2$ aggregated GNPs is less than half of that of $CuSO_4$ aggregated; (b) SERS spectra of $CuSO_4$ and $MgCl_2$ aggregated GNPs. The former exhibit at least 5 larger SERS intensity than that of GNPs aggregation based on $MgCl_2$. Inset shows the relative intensity magnitude of the SERS signals at 1509 cm^{-1} peak.[48]

min. Huh et al.[104] proposed a novel optofluidic SERS detection chip for the detection of biomolecules with electrokinetically active microwells. The chip increases the aggregation of gold colloids and sample concentration for greater detection sensitivity by a combination of electrokinetic effects. In this measurement, 44-nm carboxylate functionalized fluorescent polystyrene is introduced into the chip through the inlet port to quantify the capability of this device before application of the electric field between the upper and lower gold electrodes to attracting the nanoparticles onto the microwell. Figure 18 depicts the images of the aggregation of 44-nm polystyrene at an applied potential of 1 V between the upper electrode and well bottom for 2.5 s. This new approach using the electrokinetically active microwells not only provides efficient solution mixing between the target nucleic acids and Raman enhancers but also leads to colloid aggregation with greater detection sensitivity and reproducibility.

D. Detection of different analytes

Optofluidic devices provide many benefits in SERS detection such as efficient mixing, strong aggregation of metal nanoparticles, and fast reactions thus enabling the acquisition of stable and sensitive SERS signals even at low analyte concentrations. In addition, the ease in switching different analytes is another benefit of the SERS based optofluidic system boding well for detection of different analytes in multiple assays.

Tong et al. have developed optimized SERS detection of different types of organic analytes absorbed onto the optically aggregated silver nanoparticles in a microfluidic

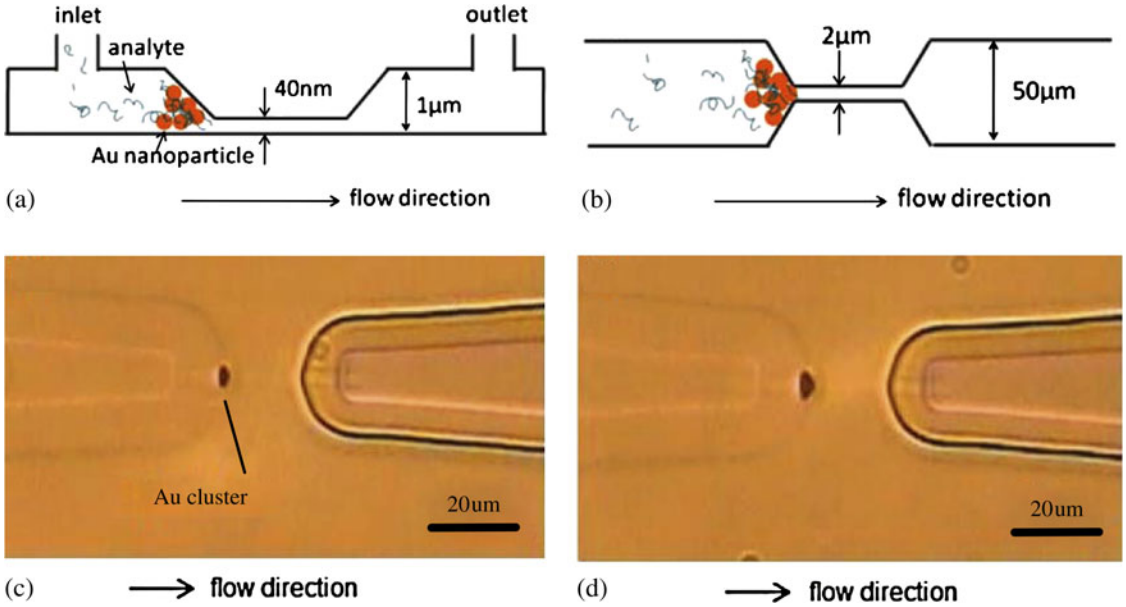

FIG. 17. (a, b) Schematic diagram of the optofluidic device at the side view and top view; (c, d) optical microscopic images showing aggregation of GNPs in an optofluidic device, 3 min after adding sample and 12 min after adding sample.[103]

device. Here, the focused near infrared laser beam traps and aggregates Ag nanoparticles at the bottom of the channel producing efficient SERS enhancers. At the same time, a separate green laser is used for Raman excitation. As shown in Fig. 19(a), thiophenol (TP) and 2-naphthalenethiol (2-NT) solutions are separated by air gaps in the right tube.[105] Ag colloids acting as the SERS enhancers are transferred to the other tube sequentially under the force of the pump. It is in the T-connector where mixing of the analytes and metal nanoparticles occurs. Figure 19(b) displays the SERS spectra of TP and 2-NT obtained from the optically aggregated Ag nanoparticles in the microfluidic channel. Using this novel system, fast and high-sensitivity sequential detection of two different analytes in the input tube can be achieved.

V. SUMMARY AND FUTURE DEVELOPMENT PROSPECTS

By incorporating the SERS detection technique into flow cells with micro- or nanochannels in an optofluidic system, various analyses such as chemical reactions, biological analysis, and environmental detection can be carried out in a convenient way even at low concentrations. In the microfluidic channels, small volumes are required and so dangerous chemical reactions as well as associated monitoring and feedback can be implemented relatively safely. Environmental pollution caused by industrial waste is harmful to human health. Therefore, accurate detection is demanded and a fast and sensitive method using real-time sensing systems for environmental monitoring, forensic science, and homeland defense applications can be realized by conducting SERS in optofluidic devices.[106]

In this review, we focused on the advantages of optofluidic devices in which micro- or nanofluidics/SERS detection systems have been developed. Problems associated with the poor reproducibility due to different particle size and inhomogeneous aggregation of metal nanoparticles in the solution and solid SERS-active substrates can be solved by conducting SERS from micro- or nanochannels. It is possible to conduct rapid analysis with efficient mixing instead of the time consuming reactions inherent to SERS performed under regular conditions. In addition, efficient mixing of samples can be

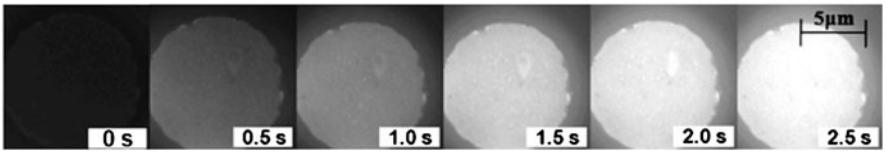

FIG. 18. Schematic images of sample aggregation of 44-nm polystyrene from the bulk solution into the channel at an applied potential of 1 V between the upper electrode and the bottom of the well for 2.5 s.[104]

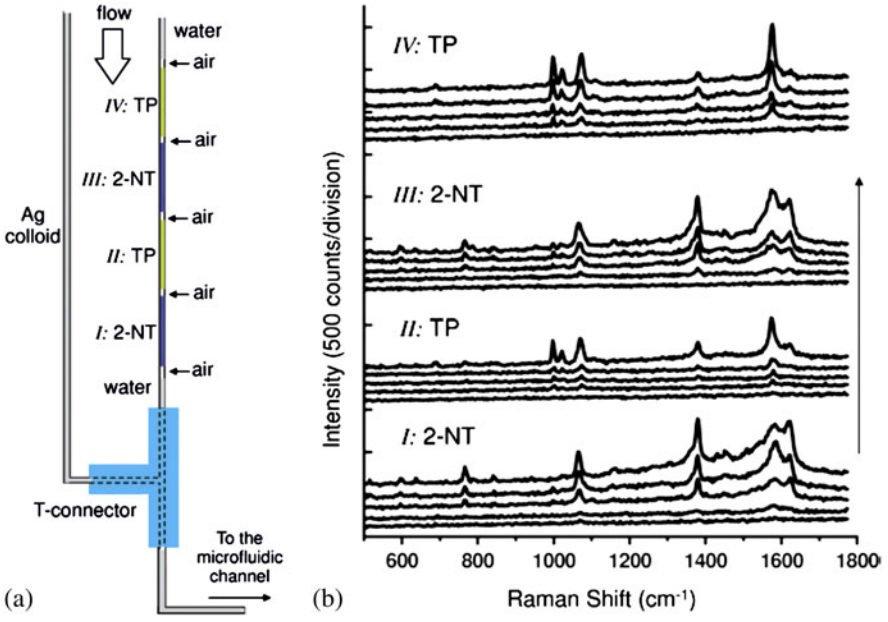

FIG. 19. Consecutive detection of two different molecules. (a) Scheme of the configuration. (b) Time series of SERS spectra from 2-NT and TP sequentially recorded as silver nanoparticles incubated with corresponding thiols, flow into the microfluidic channel and become optically aggregated. The flow rate was 1.0 mL/min and the integration time was 3 s.[105]

achieved by using optimally designed channels to manipulate the fluid. Memory effects caused by deposition of nanoparticle aggregates onto the channel surfaces in the microfluidic chips can be prevented by the droplet-based two-phase liquid/liquid segmented flow. We also discussed the efficient and stable aggregation of metal nanoparticles to improve the detection reproducibility and intensity. Furthermore, the ability to operate within a continuous flow regime and to generate homogeneous mixing conditions in the microfluidic channels makes reliable quantitative SERS-based analysis relatively straightforward compared to conventional SERS. SERS is closely linked to nanoscience and recent results suggest that highly reproducible and inexpensive SERS-active substrates can be integrated into optofluidic systems. In fact, a highly integrated optofluidic chip with multiple functions and small size are required for future diagnostics and nanobiology.

ACKNOWLEDGMENTS

This work was jointly supported by the National Natural Science Foundation of China under Grant No. 50801013, Natural Science Foundation of Jiangsu Province, China under Grant No. BK2009291, Specialized Research Fund for the Doctoral Program of Higher Education under Grant No. 200802861065, Excellent Young Teachers Program of Southeast University, Hong Kong Research Grants Council (RGC) General Research Fund (GRF) No. CityU 112307, and City University of Hong Kong Strategic Research Grant (SRG) No. 7008009.

REFERENCES

1. E. Smith and G. Dent: *Modern Raman Spectroscopy-A Practical Approach* (John Wiley & Sons Ltd., West Sussex, England, 2005).
2. B. Schrader: *Infrared and Raman Spectroscopy* (VCH, Weinheim, Germany, 1995).
3. C.V. Raman and K.S. Krishnan: A new type of secondary radiation. *Nature* **121**, 501 (1928).
4. M. Schmitt and J. Popp: Raman spectroscopy at the beginning of the twenty-first century. *J. Raman Spectrosc.* **37**, 20 (2006).
5. M. Fleischmann, P.J. Hendra, and A.J. McQuillan: Raman spectra of pyridine adsorbed at a silver electrode. *Chem. Phys. Lett.* **26**, 163 (1974).
6. Y.S. Huh, A.J. Chung, and D. Erickson: Surface enhanced Raman spectroscopy and its application to molecular and cellular analysis. *Microfluid. Nanofluid.* **6**, 285 (2009).
7. D.L. Jeanmaire and R.P. Van Duyne: Surface Raman spectroelectrochemistry. *J. Electroanal. Chem.* **84**, 1 (1977).
8. S. Chan, S. Kwon, T.W. Koo, L.P. Lee, and A.A. Berlin: Surface-enhanced Raman scattering of small molecules from silver-coated silicon nanopores. *Adv. Mater.* **15**, 1595 (2003).
9. W.E. Doering and S. Nie: Spectroscopic tags using dye-embedded nanoparticles and surface-enhanced Raman scattering. *Anal. Chem.* **75**, 6171 (2003).
10. S.P. Mulvaney, M.D. Musick, C.D. Keating, and M.J. Natan: Glass-coated, analyte-tagged nanoparticles: A new tagging system based on detection with surface-enhanced Raman scattering. *Langmuir* **19**, 4784 (2003).
11. N.R. Jana: Silver coated gold nanoparticles as new surface enhanced Raman substrate at low analyte concentration. *Analyst (Lond.)* **128**, 954 (2003).
12. K. Kneipp, H. Kneipp, I. Itzkan, R.R. Dasari, and M.S. Feld: Ultrasensitive chemical analysis by Raman spectroscopy. *Chem. Rev.* **99**, 2957 (1999).
13. Y. Xu, J. Wu, W. Sun, D. Tao, L. Yang, Z. Song, S. Weng, Z. Xu, R.D. Soloway, D. Xu, and G. Xu: A new mechanism of Raman enhancement and its application. *Chemistry* **8**, 5323 (2002).
14. P. Kambhampati, A. Campion, and O.K. Song: Probing photoinduced charge transfer at atomically smooth metal surfaces using surface-enhanced Raman scattering. *Phys. Status Solidi A: Appl. Res.* **75**, 233 (1999).
15. T. Qiu, W.J. Zhang, and P.K. Chu: Recent progress in fabrication of anisotropic nanostructures for surface-enhanced Raman spectroscopy. *Recent Pat. Nanotechnol.* **3**, 10 (2009).
16. M. Moskovits: Surface enhanced spectroscopy. *Rev. Mod. Phys.* **57**, 783 (1985).
17. M. Moskovits: Surface-enhanced Raman spectroscopy: A brief retrospective. *J. Raman Spectrosc.* **36**, 485 (2005).
18. L. Chen and J. Choo: Recent advances in surface-enhanced Raman scattering detection technology for microfluidic chips. *Electrophoresis* **29**, 1815 (2008).
19. J. Ni, R.J. Lipert, G.B. Dawson, and M.D. Porter: Immunoassay readout method using extrinsic Raman labels adsorbed on immunogold colloids. *Anal. Chem.* **71**, 4903 (1999).
20. K. Kneipp, Y. Wang, and H. Kneipp: Single molecule detection using surface-enhanced Raman scattering (SERS). *Phys. Rev. Lett.* **78**, 1667 (1997).
21. K. Kneipp, H. Kneipp, and V.B. Kartha: Detection and identification of a single DNA base molecule using surface-enhanced Raman scattering (SERS). *Phys. Rev. E: Stat. Phys., Plasmas, Fluids, Relat. Interdiscip. Top.* **57**, 6281 (1998).
22. S. Nie and R.S. Emory: Probing single molecules and single nanoparticles by surface-enhanced Raman scattering. *Science* **275**, 1102 (1997).
23. G.T. Taylor, S.K. Sharma, and K. Mohanan: Optimization of a flow-injection sampling system for quantitative-analysis of dilute aqueous-solutions using combined resonance and surface-enhanced Raman-spectroscopy (SERRS). *Appl. Spectrosc.* **44**, 635 (1990).
24. J.J. Laserna: Combining fingerprinting capability with trace analytical detection: Surface-enhanced Raman spectrometry. *Anal. Chim. Acta* **283**, 607 (1993).
25. L. He, M.J. Natan, and C.D. Keating: Surface-enhanced Raman scattering: A structure-specific detection method for capillary electrophoresis. *Anal. Chem.* **72**, 5438 (2000).
26. P.A. Walker, M.D. Morris, M.A. Burns, and B.N. Johnson: Isotachophoretic separations on a microchip: Normal Raman spectroscopy detection. *Anal. Chem.* **70**, 3766 (1998).
27. R.M. Connatser, M. Cochran, R.J. Harrison, and M.J. Sepaniak: Analytical optimization of nanocomposite surface-enhanced Raman spectroscopy/scattering detection in microfluidic separation devices. *Electrophoresis* **29**, 1441 (2008).
28. A. Dölle, M.A. Suhm, and H.J. Weingärtner: Anisotropic molecular reorientation of liquid benzene revisited. A study using ^{13}C magnetic relaxation through chemical shift anisotropy and spin rotation. *J. Chem. Phys.* **94**, 3361 (1991).
29. K. Kneipp, H. Kneipp, R. Manoharan, E.B. Hanlon, I. Itzkan, R.R. Dasari, and M.S. Feld: Extremely large enhancement factors in surface-enhanced Raman scattering for molecules on colloidal gold clusters. *Appl. Spectrosc.* **52**, 1493 (1998).
30. A. Chehaidar, R. Carles, A. Zwick, C. Meunier, B. Cros, and J. Durand: Chemical bonding analysis of *a*-SiC: H films by Raman spectroscopy. *J. Non-Cryst. Solids* **37**, 169 (1994).

31. A. Ehlert and S. Buettgenbach: Automatic sensor system for groundwater monitoring network. *Proc. SPIE* **3857**, 61 (1999).
32. D. Psaltis, S.R. Quake, and C. Yang: Developing optofluidic technology through the fusion of microfluidics and optics. *Nature* **442**, 381 (2006).
33. A. Berthod, J.J. Laserna, and J.D. Winefordner: Surface enhanced Raman spectrometry on silver hydrosols studied by flow-injection analysis. *Appl. Spectrosc.* **41**, 1137 (1987).
34. A. Manz, D.J. Harrison, E.M. Verpoorte, J.C. Fettinger, A. Paulus, H. Lüdi, and H.M. Widmer: Planar chips technology for miniaturization and integration of separation techniques into monitoring systems-capillary electrophoresis on a chip. *J. Chromatog*. **593**, 253 (1992).
35. T. Park, S. Lee, G.H. Seong, J. Choo, E.K. Lee, Y.S. Kim, W.H. Ji, S.Y. Hwang, D.G. Gweon, and S. Lee: Highly sensitive signal detection of duplex dye-labelled DNA oligonucleotides in a PDMS microfluidic chip: Confocal surface-enhanced Raman spectroscopic study. *Lab Chip* **5**, 437 (2005).
36. P.C. Lee and D. Meisel: Adsorption and surface-enhanced Raman of dyes on silver and gold sols. *J. Phys. Chem.* **86**, 3391 (1982).
37. N. Leopold and B. Lendl: A new method for fast preparation of highly surface-enhanced Raman scattering (SERS) active silver colloids at room temperature by reduction of silver nitrate with hydroxylamine hydrochloride. *J. Phys. Chem. B* **107**, 5723 (2003).
38. L. Gunnarsson, E.J. Bjerneld, H. Xu, S. Petronis, B. Kasemo, and M. Käll: Interparticle coupling effects in nanofabricated substrates for surface-enhanced Raman scattering. *Appl. Phys. Lett.* **78**, 802 (2001).
39. L.A. Dick, A.D. McFarland, C.L. Haynes, and R.P. Van Duyne: Metal film over nanosphere (MFON) electrodes for surface-enhanced Raman spectroscopy (SERS): Improvements in surface nanostructure stability and suppression of irreversible loss. *J. Phys. Chem. B* **106**, 853 (2002).
40. K. Faulds, D. Graham, and W.E. Smith: Evaluation of surface-enhanced resonance Raman scattering for quantitative DNA analysis. *Anal. Chem.* **76**, 412 (2004).
41. H. Wang, C.S. Levin, and N.J. Halas: Nanosphere arrays with controlled sub-10-nm gaps as surface-enhanced Raman spectroscopy substrates. *J. Am. Chem. Soc.* **127**, 14992 (2005).
42. I.M. White, H. Oveys, and X. Fan: Liquid core optical ring resonator sensors. *Opt. Lett.* **31**, 1319 (2006).
43. F.T. Docherty, P.B. Monaghan, R. Keir, D. Graham, W.E. Smith, and J.M. Cooper: The first SERRS multiplexing from labelled oligonucleotides in a microfluidics lab-on-a-chip. *Chem. Commun.* **1**, 118 (2004).
44. I.M. White, J. Gohring, and X. Fan: SERS-based detection in an optofluidic ring resonator platform. *Opt. Express* **15**, 17434 (2007).
45. P. Measor, L. Seballos, D. Yin, and J.Z. Zhang: On-chip surface-enhanced Raman scattering detection using integrated liquid-core waveguides. *Appl. Phys. Lett.* **90**, 211107 (2007).
46. I.M. White, S.I. Shapova, H. Zhu, J.D. Suter, S. Lacey, P. Zhang, H. Oveys, L. Brewington, J. Gohring, and X. Fan: Applications of the liquid core optical ring resonator platform. *Proc. SPIE* **6757**, 675707 (2007).
47. Y.S. Huh and D. Erickson: Aptamer based surface-enhanced Raman scattering detection of vasopressin using multilayer nanotube arrays. *Biosens. Bioelectron.* **25**, 1240 (2010).
48. D. Choi, T. Kang, H. Cho, Y. Choi, and L.P. Lee: Additional amplifications of SERS via an optofluidic CD-based platform. *Lab Chip* **9**, 239 (2009).
49. H. Becker and C. Gartner: Polymer microfabrication methods for microfluidic analytical applications. *Electrophoresis* **21**, 12 (2000).
50. J.M. Ng, I. Gitlin, A.D. Stroock, and G.M. Whitesides: Components for integrated poly(dimethylsiloxane) microfluidic systems. *Electrophoresis* **23**, 3461 (2002).
51. H. Becker and L.E. Locascio: Polymer microfluidic devices. *Talanta* **56**, 267 (2002).
52. A.J. deMello: Control and detection of chemical reactions in microfluidic systems. *Nature* **442**, 394 (2006).
53. S.K. Sia and G.M. Whitesides: Microfluidic devices fabricated in poly(dimethylsiloxane) for biological studies. *Electrophoresis* **24**, 3563 (2003).
54. N. Ohnishi, W. Satoh, K. Morimoto, J. Fukuda, and H. Suzuki: Automatic electrochemical sequential processing in a microsystem for urea detection. *Sens. Actuators, B: Chem.* **144**, 146 (2010).
55. E.R. Choban, L.J. Markoski, A. Wieckowski, and P.J.A. Kenis: Microfluidic fuel cell based on laminar flow. *J. Power Sources* **128**, 54 (2004).
56. N. Kockmann, J. Kastner, and P. Woias: Reactive particle precipitation in liquid microchannel flow. *Chem. Eng. J.* **135**, 110 (2008).
57. D. Lee, S. Lee, G.H. Seong, J. Choo, E.K. Lee, D.G. Gweon, and S. Lee: Quantitative analysis of methyl parathion pesticides in a polydimethylsiloxane microfluidic channel using confocal surface-enhanced raman spectroscopy. *Appl. Spectrosc.* **60**, 373 (2006).
58. L.X. Quang, C. Lim, G.H. Seong, J. Choo, K.J. Dob, and S.K. Yoo: A portable surface-enhanced Raman scattering sensor integrated with a lab-on-a-chip for field analysis. *Lab Chip* **8**, 2214 (2008).
59. D.J. Kim, H.J. Oh, T.H. Park, J.B. Choo, and S.H. Lee: An easily integrative and efficient micromixer and its application to the spectroscopic detection of glucose-catalyst reactions. *Analyst (Lond.)* **130**, 293 (2005).
60. R.H. Liu, J. Yang, M.Z. Pindera, M. Athavale, and P. Grodzinski: Bubble-induced acoustic micromixing. *Lab Chip* **2**, 151 (2002).
61. M.H. Oddy, J.G. Santiago, and J.C. Mikkelsen: Electrokinetic instability micromixing. *Anal. Chem.* **73**, 5822 (2001).
62. Y. Wang, H. Chen, S. Dong, and E. Wang: Surface-enhanced Raman scattering of silver-gold bimetallic nanostructures with hollow interiors. *J. Chem. Phys*. **125**, 044710 (2006).
63. S.H. Lee, K.C. Bantz, N.C. Lindquist, S.H. Oh, and C.L. Haynes: Self-assembled plasmonic nanohole arrays. *Langmuir* **25**, 13685 (2009).
64. Z. Luo, W. Yang, A. Peng, Y. Ma, H. Fu, and J. Yao: Net-like assembly of Au nanoparticles as a highly active substrate for surface-enhanced Raman and infrared spectroscopy. *J. Phys. Chem. A* **113**, 2467 (2009).
65. T. Kang, I. Yoon, J. Kim, H. Ihee, and B. Kim: Au nanowire–Au nanoparticles conjugated system which provides micrometer size molecular sensors. *Chemistry* **16**, 1351 (2010).
66. T. Qiu, X.L. Wu, J.C. Shen, and P.K. Chu: Silver nanocrystal superlattice coating for molecular sensing by surface-enhanced Raman spectroscopy. *Appl. Phys. Lett.* **89**, 131914 (2006).
67. T. Qiu, W.J. Zhang, X.Z. Lang, Y.J. Zhou, T.J. Cui, and P.K. Chu: Controlled assembly of highly Raman-enhancing silver nanocap arrays templated by porous anodic alumina membranes. *Small* **5**, 2333 (2009).
68. M. Fan and A.G. Brolo: Silver nanoparticles self assembly as SERS substrates with near single molecule detection limit. *Phys. Chem. Chem. Phys.* **11**, 7381 (2009).
69. D.R. Ward, N.K. Grady, C.S. Levin, N.J. Halas, Y.P. Wu, P. Nordlander, and D. Natelson: Electromigrated nanoscale gaps for surface-enhanced Raman spectroscopy. *Nano Lett.* **7**, 1396 (2007).
70. Q. Min, M.J.L. Santos, E.M. Girotto, A.G. Brolo, and R. Gordon: Localized Raman enhancement from a double-hole nanostructure in a metal film. *J. Phys. Chem. C* **112**, 15098 (2008).
71. M. Sackmann, S. Bom, T. Balster, and A. Materny: Nanostructured gold surfaces as reproducible substrates for surface-enhanced Raman spectroscopy. *J. Raman Spectrosc.* **38**, 277 (2007).

72. W.F. Nirode, G.L. Devault, M.J. Sepaniak, and R.O. Cole: On-column surface-enhanced Raman spectroscopy detection in capillary electrophoresis using running buffers containing silver colloidal solutions. *Anal. Chem.* **72**, 1866 (2000).
73. R.M. Connatser, M. Cochran, R.J. Harrison, and M.J. Sepaniak: Analytical optimization of nanocomposite surface-enhanced Raman spectroscopy/scattering detection in microfluidic separation devices. *Electrophoresis* **29**, 1441 (2008).
74. W.E. Smith, K. Faulds, and D. Graham: Quantitative surface-enhanced resonance Raman spectroscopy for analysis. *Top. Appl. Phys.* **103**, 381 (2006).
75. S.E. Bell and N.M. Sirimuthu: Quantitative surface-enhanced Raman spectroscopy. *Chem. Soc. Rev.* **37**, 1012 (2008).
76. K.R. Ackermann, T. Henkel, and J. Popp: Quantitative online detection of low-concentrated drugs via a SERS microfluidic system. *ChemPhysChem* **8**, 2665 (2007).
77. R. Tantra, R.J. Brown, and M.J. Milton: Strategy to improve the reproducibility of colloidal SERS. *J. Raman Spectrosc*. **38**, 1469 (2007).
78. C. McLaughlin, D. MacMillan, C. McCardle, and W.E. Smith: Quantitative analysis of mitoxantrone by surface-enhanced resonance Raman scattering. *Anal. Chem.* **74**, 3160 (2002).
79. D. Cialla, U. Hubner, H. Schneidewind, R. Moller, and J. Popp: Probing innovative microfabricated substrates for their reproducible SERS activity. *ChemPhysChem* **9**, 758 (2008).
80. M.J.A. Canada, A.R. Medina, J. Frank, and B. Lendl: Bead injection for surface enhanced Raman spectroscopy: Automated on-line monitoring of substrate generation and application in quantitative analysis. *Analyst (Lond.)* **127**, 1365 (2002).
81. A. Marz, K.R. Ackermann, D. Malsch, T. Bocklitz, and T.H. Popp: Towards a quantitative SERS approach-online monitoring of analytes in a microfluidic system with isotope-edited internal standards. *J. Biophoton*. **2**, 232 (2009).
82. J.H. Jung, J. Choo, D.J. Kim, and S. Lee: Quantitative determination of nicotine in a PDMS microfluidic channel using surface enhanced Raman spectroscopy. *Bull. Korean Chem. Soc.* **27**, 277 (2006).
83. S. Lee, J. Choi, L. Chen, B. Park, J.B. Kyong, G.H. Seong, J. Choo, Y. Lee, K.H. Shin, E.K. Lee, S.W. Joo, and K.H. Lee: Fast and sensitive trace analysis of malachite green using a surface-enhanced Raman microfluidic sensor. *Anal. Chim. Acta* **590**, 139 (2007).
84. B. Bose, L. Motiwale, and K.V.K. Rao: DNA damage and G2/M arrest in Syrian hamster embryo cells during Malachite green exposure are associated with elevated phosphorylation of ERK1 and JNK1. *Cancer Lett.* **230**, 260 (2005).
85. A. Stammati, C. Nebbia, I. De Angelis, A.G. Albo, M. Carletti, C. Rebecchi, F. Zampaglioni, and M. Dacasto: Effects of malachite green (MG) and its major metabolite, leucomalachite green (LMG), in two human cell lines. *Toxicol. In Vitro* **19**, 853 (2005).
86. A. Huebner, M. Srisa-Art, D. Holt, C. Abell, F. Hollfelder, A.J. deMello, and J.B. Edel: Quantitative detection of protein expression in single cells using droplet microfluidics.: *Chem. Commun. (Camb.)* **12**, 1218 (2007).
87. M. Srisa-Art, A.J. deMello, and J.B. Edel: High-throughput DNA droplet assays using picoliter reactor volumes. *Anal. Chem.* **79**, 6682 (2007).
88. A. Huebner, S. Sharma, M. Srisa-Art, F. Hollfelder, J.B. Edel, and A.J. deMello: Microdroplets: A sea of applications? *Lab Chip* **8**, 1244 (2008).
89. M. Srisa-Art, I.C. Bonzani, A. Williams, M.M. Stevens, A.J. deMello, and J.B. Edel: Identification of rare progenitor cells from human periosteal tissue using droplet microfluidics. *Analyst (Lond.)* **134**, 2239 (2009).
90. M. Srisa-Art, A.J. deMello, and J.B. Edel: High-throughput confinement and detection of single DNA molecules in aqueous microdroplets. *Chem. Commun. (Camb.)* **43**, 6548 (2009).
91. M. Srisa-Art, D.K. Kang, J. Hong, H. Park, R.J. Leatherbarrow, J.B. Edel, S.I. Chang, and A.J. deMello: Analysis of protein–protein interactions by using droplet-based microfluidics. *ChemBioChem* **10**, 1605 (2009).
92. K.R. Strehle, D. Cialla, P. Rosch, T. Henkel, M. Kohler, and J. Popp: A reproducible surface-enhanced Raman spectroscopy approach: Online SERS measurements in a segmented microfluidic system. *Anal. Chem.* **79**, 1542 (2007).
93. G. Wang, C. Lim, L. Chen, H. Chon, J. Choo, J. Hong, and A.J. deMello: Surface-enhanced Raman scattering in nanoliter droplets: Towards high-sensitivity detection of mercury (II) ions. *Anal. Bioanal. Chem.* **394**, 1827 (2009).
94. C.G. Blatchford, J.R. Campbell, and J.A. Creighton: Plasma resonance-enhanced Raman-scattering by adsorbates on gold colloids: The effects of aggregation. *Surf. Sci.* **120**, 435 (1982).
95. O. Siiman, L.A. Bumm, R. Callaghan, C.G. Blatchford, and M. Kerker: Surface-enhanced Raman scattering by citrate on colloidal silver. *J. Phys. Chem.* **87**, 1014 (1983).
96. S.R. Emory, R.A. Jensen, T. Wenda, M. Han, and S.M. Nie: Re-examining the origins of spectral blinking in single-molecule and single-nanoparticle SERS. *Faraday Discuss.* **132**, 249 (2006).
97. A.D. McFarland, M.A. Young, J.A. Dieringer, and R.P. Van Duyne: Wavelength-scanned surface-enhanced Raman excitation spectroscopy. *J. Phys. Chem. B* **109**, 11279 (2005).
98. M. Cyrankiewicz, T. Wybranowski, and S. Kruszewski: Study of SERS efficiency of metallic colloidal systems. *J. Phys.: Conf. Ser.* **79**, 012013 (2007).
99. Y. Yang, S. Matsubara, M. Nogamia, and J. Shi: Controlling the aggregation behavior of gold nanoparticles. *Mater. Sci. Eng., B* **140**, 172 (2007).
100. A.M. Schwartzberg, C.D. Grant, A. Wolcott, C.E. Talley, T.R. Huser, R. Bogomolni, and J.Z. Zhang: Unique gold nanoparticle aggregates as a highly active surface-enhanced Raman scattering substrate. *J. Phys. Chem. B* **108**, 19191 (2004).
101. J.D. Guingab, B. Lauly, B.W. Smith, N. Omenetto, and J.D. Winefordner: Stability of silver colloids as substrate for surface enhanced Raman spectroscopy detection of dipicolinic acid. *Talanta* **74**, 271 (2007).
102. C.C. Busby and J.A. Creighton: Efficient gold and silver electrodes for surface enchanced Raman spectral studies of electrochemical systems: The behavior of pyridine and naphthalene adsorbed on roughened gold electrodes. *J. Electroanal. Chem.* **140**, 379 (1982).
103. M. Wang, M. Benford, N. Jing, G. Cote, and J. Kameoka: Optofluidic device for ultra-sensitive detection of proteins using surface-enhanced Raman spectroscopy. *Microfluid. Nanofluid.* **6**, 411 (2009).
104. Y.S. Huh, A.J. Chung, B. Cordovez, and D. Erickson: Enhanced on-chip SERS based biomolecular detection using electrokinetically active microwells. *Lab Chip* **9**, 433 (2008).
105. L. Tong, M. Righini, M.U. Gonzalez, R. Quidantb, and M. Käll: Optical aggregation of metal nanoparticles in a microfluidic channel for surface-enhanced Raman scattering analysis. *Lab Chip* **9**, 193 (2009).
106. C. Lim, J. Hong, B.G. Chung, A.J. deMello, and J. Choo: Optofluidic platforms based on surface-enhanced Raman scattering. *Analyst (Lond.)* **135**, 837 (2010).